A NEW UNCOOLED THERMAL IR DETECTOR USING SILICON DIODE

Jae-Kwan Kim* **and Chul-Hi Han**

Department of Electrical Engineering,
Korea Advanced Institute of Science and Technology (**KAIST**),
373-1 Kusong-dong, Yusong-gu, Taejon 305-701, Korea
e-mail: hitch@cais.kaist.ac.kr, Tel.: +82-42-869-5444
*also with Samsung Electronics Co. Ltd., Korea

ABSTRACT

A new thermal infrared detector using temperature characteristics of a diode is proposed and developed. Micromachined isolated silicon diode for IR detection (MISIR) utilizes electrochemical etching technique to achieve the thermal isolation of the diode. Very high dependence on the junction temperature of the diode enables high responsivity of the MISIR and electrochemical etching provides effective isolation with simple and low-cost process. The fabricated MISIR exhibits the detectivity of 1.2×10^{10} (cm·Hz$^{1/2}$/W) under air ambient at room temperature.

INTRODUCTION

Infrared (IR) imaging systems extends human vision beyond the red into the far IR by making the patterns of thermal radiation visible. Among IR detectors, thermal IR detectors [1-2] can be operated in room temperature without expensive cryogenic cooler, which makes them suitable for many applications. Thermal IR detectors have two inherent weak points: low detectivity and slow response. Slow response can be overcome by integration of many detectors on a focal plane. The advent of focal plane array (FPA) provides the ground for the application of thermal detector to IR imaging systems. But the low detectivity excludes the thermal IR detectors from many potential applications.

Two major issues of thermal IR detector are thermal isolation and temperature sensing mechanism. To enhance responsivity, thermal conductance as low as possible is required. Also high sensitive temperature sensing mechanism results in responsivity improvement.

Silicon p-n diodes have been used for temperature sensors due to the linearity between the junction voltage and the junction temperature at a constant current [3]. On the contrary, the current at a fixed bias voltage changes exponentially as the junction temperature changes. In ambient IR detection – human, natural scene, car, and building, the temperature of the IR detector hardly change more than a few degrees. Such a small temperature range, the exponential relationship between diode current and temperature can be regarded as linear steeper than that of the diode voltage.

In respect of the thermal isolation, larger gap between the detector structure and substrate is desirable, which keeps the heat of the detector from flowing away to the substrate. Many thermal IR detectors have been fabricated with surface micromachining techniques. In the surface micromachining, the gap is limited by the thickness of sacrificial layer. Conventional methods for the thermal isolation are anisotropic silicon etchings. But the anisotropic etchings need special equipment and specific substrates for accomplishing fine and aligned silicon etch. Generally, double-side aligning and a specific crystallographic oriented wafer are required for anisotropic silicon etching.

Electrochemical etching can overcome the limit of surface micromachining because it can etch the whole substrate below detectors. Also due to its self-aligning property, the thermal isolation between pixels can be easily accomplished with very simple. In this paper, a new thermal IR detector, micromachined isolated silicon diode for IR detection (MISIR), is proposed and developed. A fabricated MISIR shows a very high detectivity of 1.2×10^{10} (cm·Hz$^{1/2}$/W) without either vacuum packaging or cryogenic cooling.

THERMAL CHARACTERISTICS OF A DIODE

Temperature dependence of the current of a semiconductor p-n junction diode has been exploited in temperature measurements [4]. One attractive feature of such a device is its well-defined temperature dependence. Another feature is that the response of the junction is set primarily by the bulk impurity distribution and tends to be quite stable [3].

As the junction temperature of a diode increases, the junction voltage also rises linearly at a constant bias current. But at a fixed junction voltage, the diode

current shows an exponential relationship with temperature. Thus, the diode current shows much higher responsivity to temperature than the junction voltage. Figure I shows measurement results of the forward current vs. temperature of a fabricated silicon diode. Diode forward current increases exponentially as temperature rises. The slope of the forward current of the diode to the temperature (decade/K) falls with increasing bias voltage.

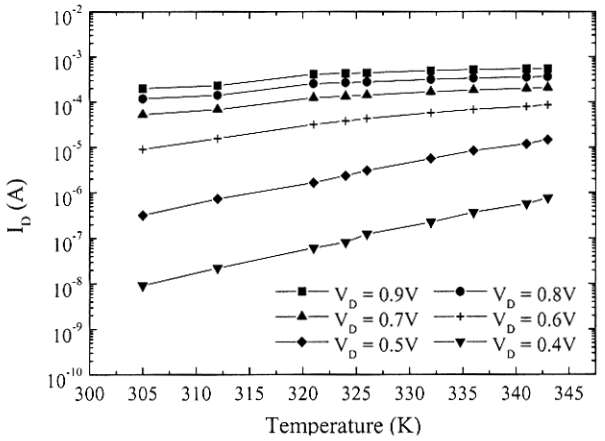

Figure I Dependence of diode current on temperature

The temperature behavior of the forward current of a p-n junction diode can be derived from the diode current equation [5].

$$I = I_0\left[\exp\left(\frac{qV}{nkT}\right)-1\right] \approx I_0\exp\left(\frac{qV}{nkT}\right) \quad for\ I >> I_0 \tag{1}$$

where I is the forward current, I_0 is the reverse saturation current, q is the electronic charge, V is the junction voltage, k is the Boltzmann's constant, n is the device ideality factor, and T is absolute temperature in K. The reverse saturation current depends on temperature by the relationship given as [6]

$$I_0 = K_1 T^{5/2}\exp\left(-\frac{qE_g}{nkT}\right) \tag{2}$$

where K_1 is a constant of the junction material and geometry and E_g is the energy bandgap. Energy bandgap E_g can be expressed as [7]

$$E_g(T) = 1.17 - \frac{\alpha T^2}{\beta + T} \quad \Rightarrow \frac{\partial E_g}{\partial T} = -\frac{\alpha T(2\beta + T)}{(\beta + T)^2} \tag{3}$$

where α is 4.73×10^{-4} and β is 636 in silicon.

As the diode current increases, the effect of the series resistance of a diode caused by silicon and metal resistance must be taken into account. As a result

$$I = K_1 T^{5/2}\exp\left[\frac{q\{(V - Ir_s) - E_g(T)\}}{nkT}\right] \tag{4}$$

where r_s is the series resistance of a diode. Assuming the temperature change of a diode is sufficiently smaller than background temperature (T), it can be inferred directly from the Equation (4).

$$\frac{\partial I}{\partial T} = \frac{\left[\frac{5}{2T} - \frac{q\{(V - Ir_s) - E_g\}}{nkT^2} - \frac{q}{nkT}\frac{\partial E_g}{\partial T}\right]I}{1 + \frac{qr_s}{nkT}I} \tag{5}$$

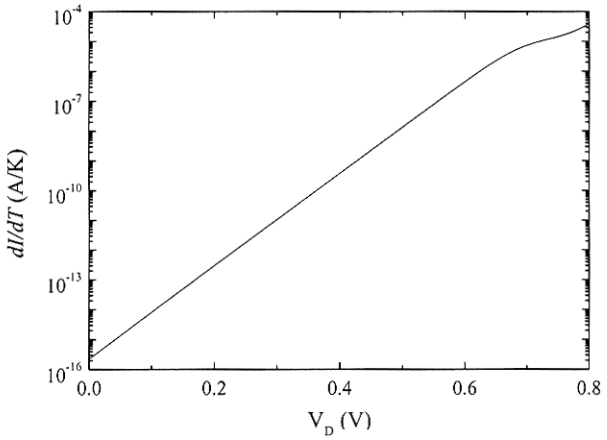

Figure II Simulation result of $\frac{\partial I}{\partial T} - V$ of a diode

Figure II shows the simulation result of Equation (5) of a silicon diode as bias voltage varies. Simulation is performed with extracted parameters from the basic diode measurement of the fabricated diode shown in figure I. Higher bias voltage causes a larger current change with respect to unit temperature rise.

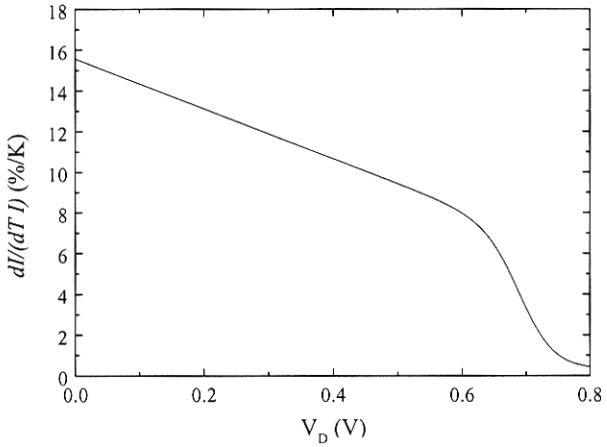

Figure III Simulation result of TCC of a diode.

Figure III shows the simulation result of $\partial I/(\partial T \cdot I)$ of the silicon diode, which can be inferred as temperature

coefficient of current (TCC) by analogy with temperature coefficient of resistance (TCR). The simulation result shows that the TCC of a diode declines with increasing bias voltage. Compared with a few tenth of TCR in metal resistor at room temperature [8], the diode current shows much higher temperature sensitivity. Comparing figure III with figure II, it can be observed that the normalized quantity, the TCC, is far less sensitive to the bias voltage.

STRUCTURES AND FABRICATIONS

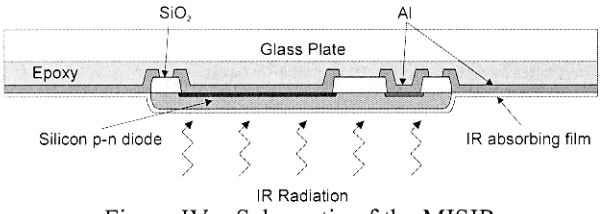

Figure IV Schematic of the MISIR

Figure IV is a schematic diagram of the MISIR. A diode for temperature sensing device is fabricated on a single crystalline silicon wafer. The fabricated wafer is attached to a glass plate to support fragile structures after electrochemical etching. Electrochemical etching is performed to remove silicon other than diode device area. By remaining only active diode areas, thermal conduction through the substrate can be eliminated. IR absorbing layer is then deposited on the backside of the devices. Each pixel and substrate are connected by thin silicon line on which metal lines for getting signal are placed.

The process starts with a boron-doped silicon wafer (100) with resistivity of 5~20 Ω·cm. After thermal oxidation of silicon by the thickness of 500Å, 2000Å thick LPCVD silicon nitride film is deposited. Silicon nitride layer is for selective impurity drive-in, which is similar to LOCOS process. Silicon nitride layer and silicon oxide are patterned by first mask step. Phosphorus diffusion (900°C, 10min) and drive-in (1100°C, 200min) is followed (figure V (a)). Impurity concentration of phosphorus diffused layer is lowered by drive-in process. Since electrochemical etching does not happen in n^--type region with a lower concentration of $10^{17}cm^{-3}$ [9], the diodes must be formed on a buried n^- layer to be protected from electrochemical etching.

Boron (975°C, 30min) and phosphorus diffusion (975°C, 30min) are performed for p-n junction and good contact with aluminum (figure V (b)). As diode current is proportional to junction area, the MISIR is designed to make the junction area as large as possible. After fabricating p-n junctions, silicon nitride film and oxide film on the areas other than diode is removed and aluminum is deposited and patterned. The aluminum patterns act as electrochemical etching electrodes, as well as electrical electrodes for n and p regions. Parts of aluminum on p-type substrate are used for electrochemical etching electrodes.

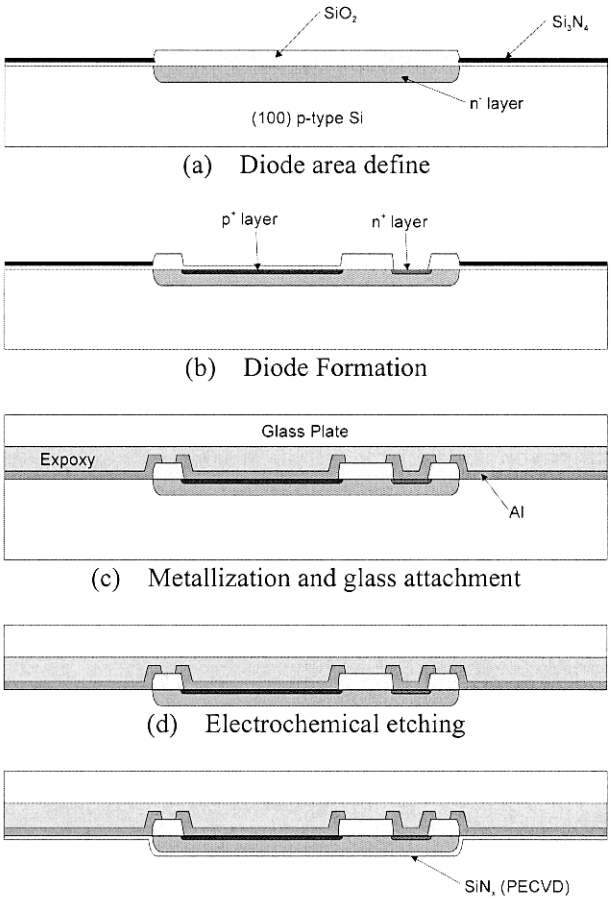

Figure V Fabrication process sequence

The substrate is attached to a glass plate using epoxy adhesive which can be cured by UV radiation (figure V (c)). The glass plate mechanically supports the fragile matrix structure during the following fabrication process. The glass plate can be substituted with a silicon substrate, a plastic plate, or anything else with mechanical hardness. Then a 2000Å thick LPCVD silicon nitride is deposited.

We have developed an electrochemical etching technique which can forms arbitrary shapes and fine patterns with self-aligned property [10-11]. As the electrochemical etching proceeds along the current path, desired etching profile and shape can be obtained by adjusting the current path. Etching patterns are formed on the front side of the substrate, but etching begins at the backside of the substrate on which no preparation is done. As etching proceeds, the etching profile converges to the etching electrode on the front side. So the double-side aligning to align the backside etching patterns to the front side patterns is not necessary.

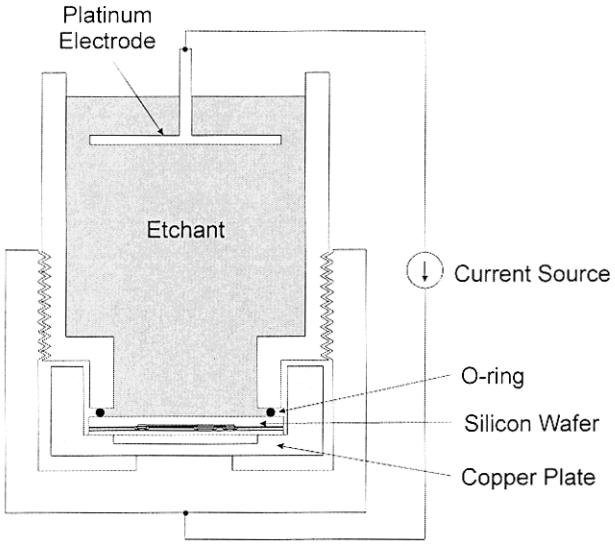

Figure VI Electrochemical etching apparatus

Electrochemical etching is performed in an apparatus as shown at figure VI. In the apparatus, only the backside of the substrate faces to etchant. By applying a current between platinum electrode and etching electrode on the substrate, electrochemical etching begins. After electrochemical etching, only silicon diode islands and aluminum interconnection lines remain, which are attached on the glass plate (figure V (d)).

A 1μm thick PECVD silicon nitride is deposited on the backside of the diode for IR absorbing layer (figure V (e)). PECVD silicon nitride is often used for IR absorbing layer in thermal detectors [12]. A measurement of PECVD silicon nitride using Fourier transform infrared spectroscopy (FTIR) reveals that its absorptance in the range of 8~12μm is about 70%.

Microphotograph of the fabricated MISIR is shown in figure VII. The size of the fabricated MISIR is 100μm×170μm. The thickness of the silicon islands is about 5μm. To enhance the responsivity, the thermal conductance of the detector must be minimized. Also the thermal capacity of the detector needs to be adjusted to meet the response time requirement. Because the active area of the pixel is defined by the system requirement – pixel pitch, and resolution, the only adjustable parameter is the thickness. In this process, the thermal capacity can be easily controlled by adjusting the thickness of the active area with the conditions of the phosphorus diffusion and the drive-in.

The fabricated MISIR has the shapes of islands connected each other with narrow and thin silicon line on which the signal line are placed. In the fabrication process, one-layer metal process is used. The signal lines have to go across some regions of the etching electrodes if the etching electrode enclose the diode completely. Therefore, the etching electrode cannot surround the diode, which leads to incomplete isolation of the pixel. But using two or more layer metallization process, complete thermal isolation can be accomplished.

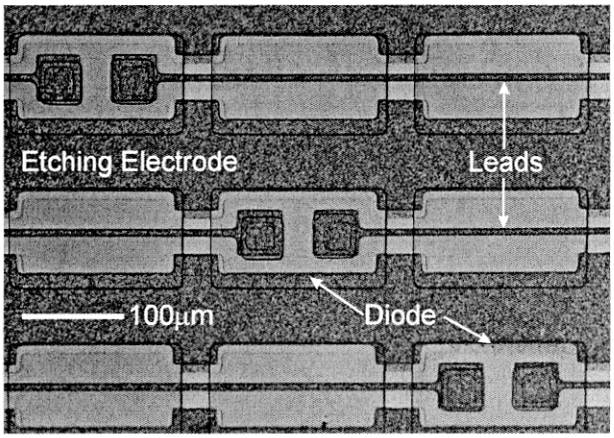

(a) Photograph of the front side of the MISIR

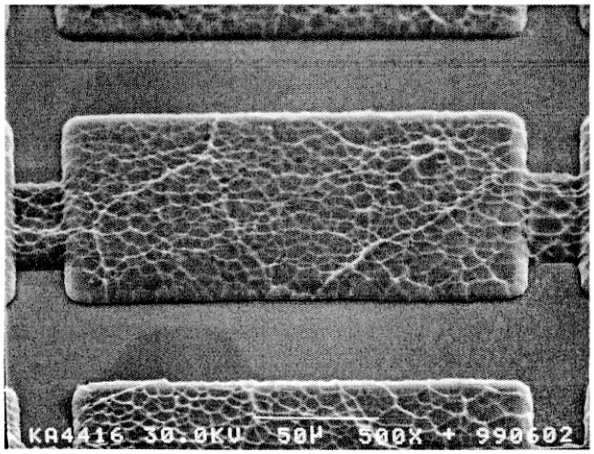

(b) SEM photograph of the backside of the MISIR

Figure VII Photographs of the fabricated MISIR

RESULTS AND DISCUSSIONS

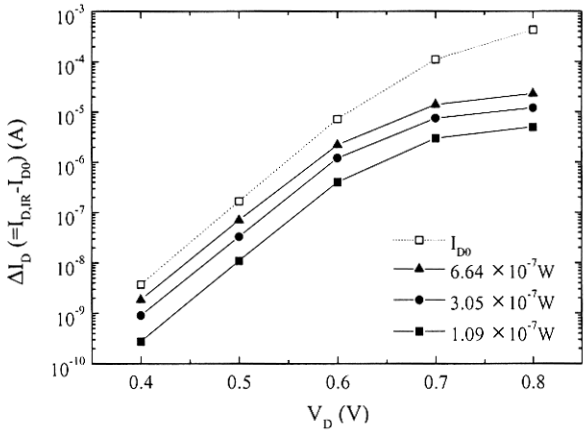

Figure VIII Change of current vs. bias voltage

Figure VIII shows the current change of the fabricated MISIR with varying incident IR power at air ambient and room temperature. IR powers have been calculated with the blackbody temperature, the aperture of the blackbody source, distance between the source and the detector, the transmittance of germanium window, and the absorptance of the silicon nitride. Each IR power corresponds to the blackbody temperature of 400, 600, and 800°C, respectively. I_{D0} and $I_{D,IR}$ mean the diode current before and after IR illumination, respectively. Current changes by IR radiation increase with the increasing bias voltage.

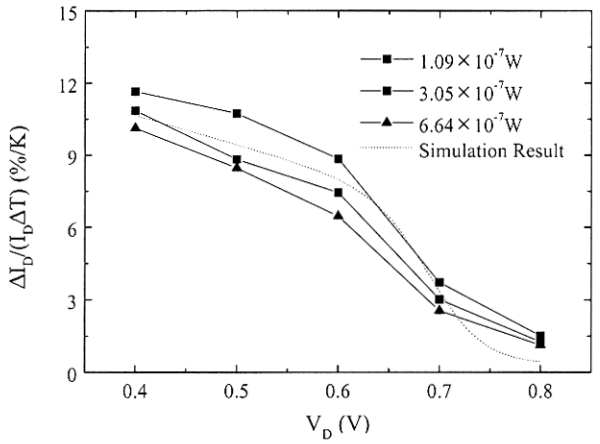

Figure IX TCC of the MISIR vs. bias voltage

The TCC of the MISIR are shown at figure IX with simulation results. The TCC falls as the bias voltage increases due to the series resistance of the diode. Increased diode current by elevated temperature flows through the series resistance. The voltage drop through the series resistance reduces the junction voltage, which makes current decrease. In a high current region, the junction voltage drop by the series resistance becomes significant. Therefore, the TCC decreases with increasing bias voltage.

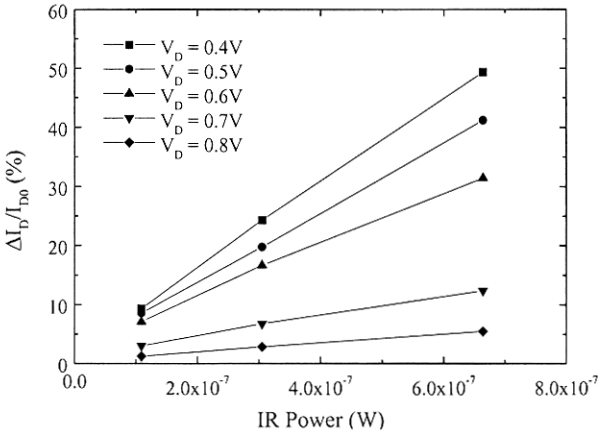

Figure X Normalized current change vs. IR power

Figure X shows the normalized current change with the bias current. The current change of the fabricated MISIR shows a good linear relationship with the incident IR power.

It has been proven that the detector has a high responsivity to IR radiation, which is due to the high sensitivity of the diode current to temperature. And the detector shows a good linear response to the incident IR power. As bias voltage increases, the magnitude of current change also increases, but the TCC decreases.

The magnitude of signal is important in the performance of detection system. Higher level of the signal makes readout circuit simple and enhances noise figure of the system. The magnitude of current change becomes larger as the bias voltage is increasing. But the measured signal has strong dependency on the diode variation and bias voltage, as well as on the temperature. The TCC has advantages in minimizing the effects of other variations except the temperature, for example, variations of device parameters, background temperature, and bias instability. Considering noise figure, responsivity and power consumption, the bias voltage must be optimized for a maximum performance.

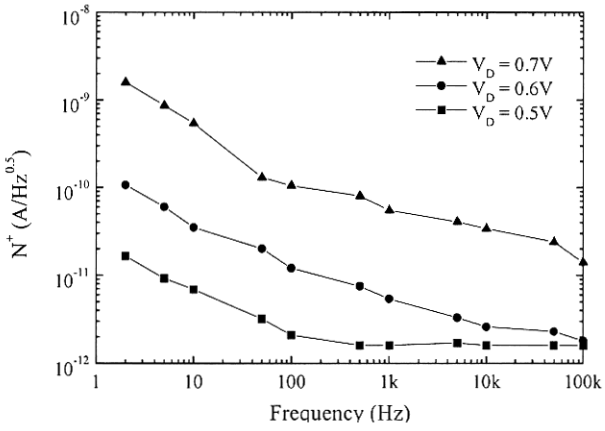

Figure XI Spectral noise current density

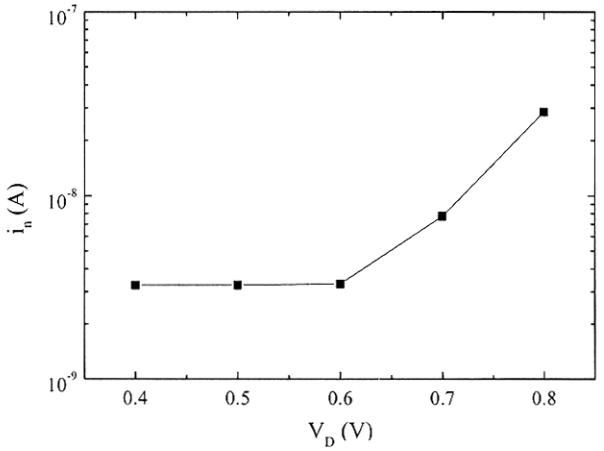

Figure XII Total noise current

In case of a diode, it is known that Johnson noise

(thermal noise), shot noise, and flicker noise (1/f noise) are dominant noise sources [13]. Spectral density of the total noise current of the MISIR is shown at figure XI. At low frequency – up to 10kHz, the flicker noise plays a dominant role. As the frequency increases, the flicker noise diminishes, and the Johnson noise and the shot noise form a constant noise level.

Assuming 64kHz of bandwidth, the calculation result of the total noise current is shown at figure XII. The flicker noise and the shot noise increase with increasing bias voltage. In the low bias voltage region up to 0.6V, the Johnson noise is dominant and bias voltage has little effect on the total noise current. But above 0.7V, the flicker noise and shot noise grow much higher than the Johnson noise leading to the increment of the total noise current.

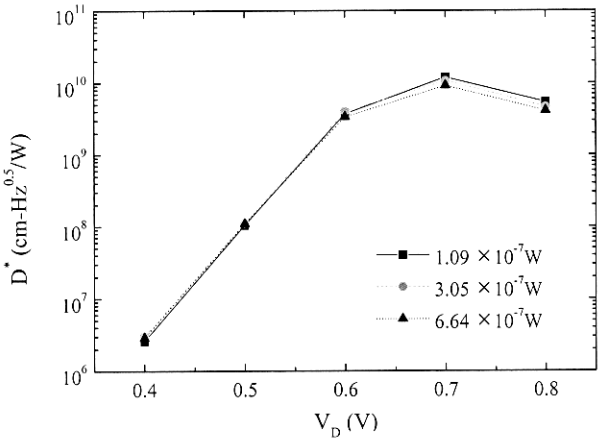

Figure XIII Detectivity of the MISIR

Figure XIII shows the detectivity of the fabricated MISIR. Detectivity has its peak at about 0.7V bias voltage. It can be explained from figure VIII and XII. Current change increases as the bias voltage grows, but the amount of increment falls. In addition, the total noise current begins to grow at about 0.7V. Therefore, the detectivity shows its peak at about 0.7V.

The fabricated MISIR shows a detectivity of 1.2×10^{10} (cm·Hz$^{1/2}$/W) at 0.7V bias voltage without either vacuum packaging or cryogenic cooling, which is the highest among the reported thermal IR detector under room temperature operation.

CONCLUSION

In this paper, we have proposed and developed a new thermal IR detector – micromachined isolated diode for IR detection (MISIR). It has a very simple structure and can be fabricated with a process compatible with conventional CMOS technology. Electrochemical etching can provide a feasible method for the thermal isolation. The MISIR shows a very high detectivity of 1.2×10^{10} (cm·Hz$^{1/2}$/W). MISIR IR imaging system is under development.

ACKNOWLEDMENTS

The authors would like to thank J. –H Kim for the name of MISIR, C. –S. Lee, Y. –S. Choi, Dr. J. –D. Lee, and Dr. J. –B. Yoon for their helpful discussions, Prof. E. –S. Yoon and Prof. C. –K. Kim for their supports and encouragements on this work, S. –H. Bae and Y –H. Kim for technical assistane in IR measurements. All members in MiDAS laboratory are also appreciated.

REFERENCES

[1] K. C. Liddard, "Starting Focal Plane Arrays for Advanced Ambient Temperature Infrared Sensors," *Proc. SPIE*, vol. 2552, p. 564, 1995

[2] D. L. Polla, C. Ye, and T. Tamagawa, "Surface-micromachined $PbTiO_3$ Pyroelectric Detectors," *Appl. Phys. Lett.*, vol. 59, p. 3539, 1991

[3] C. K. Saul, and J. N. Zemel, "Diode-based Microfabricated Hot-plate Sensor," *Sensors and Actuators A*, vol. 65, p. 128, 1998

[4] K. S. Szajda, C. G. Sodini, and H. F. Bowman, "A Low Noise, High Resolution Silicon Temperature Sensor," *IEEE J. Solid-State Circuits*, vol. 31, p. 1308, 1996

[5] C. T. Sah, R. N. Noycee, and W. Shockley, "Carrier Generation and Recombination in p-n Junction and p-n Junction Characteristics," *Proc. IRE*, vol. 45, p.1228, 1957

[6] Y. B. Acharya, and P. D. Vyacahare, "Study on the Temperature Sensing Capability of a Light-emitting Diode," *Rev. Sci. Instrum.*, vol. 68, p. 4465, 1997

[7] S. M. Sze, *Physics of Semiconductor Devices*, John Wiley & Sons, New Jersey, 1981

[8] P. W. Kruse, "Principles of Uncooled Infrared Focal Plane Arrays", *Semiconductors & Semimetals*, vol. 47, p. 17, 1997

[9] P. C. Searson, and X. G. Zhang, "The Anodic Dissolution of Silicon in HF Solution," *J. Electrochem. Soc.*, vol. 137, p. 2539, 1990

[10] H. –D. Lee, H. –J. Lee, C. –K. Kim, and C. –H. Han, "Formation of Self-aligned Holes in an Arbitrary Pattern in Silicon Substrate," *Appl. Phys. Lett.*, vol. 66, p. 3272, 1995

[11] H. –D. Lee, J. –K. Kim, and C. –H. Han, "Simultaneous and Accurate Formation of Variously Shaped Holes in Silicon Substrate," *Jpn. J. Appl. Phys.*, vol. 36, p. L529, 1997

[12] M. Mao, T. Perazzo, O. Kwon, A. Majumdar, J. Varesi, and P. Norton, "Direct-View Uncooled Micro-Optomechanical Infrared Camera," *Proc. MEMS '99*, p. 100, 1999

[13] P. R. Gray, and R. G. Meyer, *Analysis and Design of Analog* Integrated *Circuits*, John Wiley & Sons, New Jersey, 1993